VYSOKÉ UČENÍ TECHNICKÉ V BRNĚ
Fakulta strojního inženýrství
Ústav procesního inženýrství

Ing. Miroslav Rebej

SIMULACE FOTOBIOREAKTORŮ Z POHLEDU HYDRODYNAMIKY A PŘENOSU HMOTY

SIMULATIONS OF PHOTOBIOREACTORS FROM HYDRODYNAMICS AND MASS TRANSFER POINT OF VIEW

Zkrácená verze dizertační práce

Obor:	Konstrukční a Procesní Inženýrství
Školitel:	doc. Ing. Zdeněk Jegla, Ph.D.
Oponenti:	Prof. Dr.-Ing. Alexandra Jördening University of Applied Sciences Augsburg, Německo
	doc. Ing. Vojtěch Turek, Ph.D. Vysoké učení technické v Brně Brno, Česko
Datum obhajoby:	22. listopadu 2022

Keywords

Photobioreactor; multiphase flow; PIV; bubbly flow; mass transfer; fluid dynamics

Klíčová slova

Fotobioreaktor; vícefázové proudění; PIV; bublinkový tok; přestup hmoty; dynamika tekutin

Místo uložení dizertační práce

Ústav procesního inženýrství, FSI, VUT v Brně

ISBN 80-214-...

ISSN 1213-4198

CONTENTS

1 INTRODUCTION

Microalgae are naturally ecologically diverse. Due to their ability to adapt to different life conditions, they can be found growing in many biotopes, e.g., damp places or aquatic environments. The algae lack various structures that characterize land plants, such as leaves or roots, and other organs that are found in other vascular plants. However, their uniqueness comes from the presence of chlorophyll and having photosynthetic ability in a single algal cell. Therefore, algal cultivation allows for rather easy operation for biomass generation and effective genetic and metabolic research in a much shorter time period than conventional plants (Pelczar et al., 1993). Microalgae, as biological CO_2 and O_2 exchangers, can offer some biotechnological potential, as well. Examples of areas where the microalgal technology can bring some novelty may be in areas of pharmaceuticals, cosmetics, agriculture, food, or environment. Their added value may be found, for instance, in production of high value bioproducts or in reduction of CO_2 emissions, see Table 1.1 for some examples. However, utilization of such biotechnology must be based on a strong biotechnological basis and intended biomass utilization must also be taken into account when considering a technical solution.

Table 1.1 Types of microalgae and their commercial relevance[1]

Microalgae	**Application**	**Reference**
Thalassiosira weissflogii	Production of EPA and fucoxanthin	Marella and Tiwari (2020)
Chlorella vulgaris	Wastewater biotreatment	Sabeti et al. (2019)
	Production of SFA	Ramírez-López et al. (2019)
Scenedesmus obliquus	Protein extraction	Patnaik et al. (2019)
	Biodiesel production	Han et al. (2016)
Fistulifera solaris	PUFA and EPA production	Tanaka et al. (2017)
Phaeodactylum tricornutum	PUFA and EPA production	Rodolfi et al. (2017)
Chlorella protothecoides	Biodiesel production	Darpito et al. (2015)
Tetraselmis suecica	Biodiesel production	Heo et al. (2015)

There are two major technical solutions for the cultivation of microorganisms, open and closed cultivation systems. Photobioreactors, i.e., closed technical systems for microalgal cultivation, give a clear advantage over open systems, such as ponds, when

[1] EPA: eicosapentaenoic acid; PUFA: polyunsaturated fatty acid; SFA: saturated fatty acid

it comes to intensive production of high value bioproducts. Closed photobioreactors allow for cultivation under controlled conditions so that the medium does not get contaminated or lost, e.g., due to evaporation. However, cultivation processes in such photobioreactors have different operational requirements as living conditions of microalgae are often far from their natural habitat in closed vessels. The main differences may be higher cell densities in the medium resulting in issues with irradiation density and with light patterns, or different variations of pH and temperature. Moreover, due to induced flow velocities, the cells may experience constant shear stress at, or even above, potential death-levels (Pulz, 2001; Singh and Sharma, 2012).

Therefore, the design of any technical solutions needs to be evaluated for the cost-effective application and economic feasibility. Next, adequate control strategies and harvesting techniques have to be implemented to optimize the overall process yield. Nevertheless, to reach a state where optimum growth is maintained, all aspects of microalgae cultivation must be in balance, i.e. hydrodynamics, mass transfer, irradiation, and cell growth (Acién Fernández et al., 2013; Gao et al., 2018).

1.1 OBJECTIVES OF THE DISSERTATION THESIS

The aim of this thesis is to provide mathematical models of a microalgae cultivation vessel. The methodology is based on multiphase flow analyses of the photobioreactor model that integrates the reactor's hydrodynamics with principles of mass transfer.

The first part of the doctoral dissertation thesis is dedicated to the literature review that introduces the numerical modelling of multiphase flows and its application in the field of photobioreactors. Individual aspects of numerical modelling of photobioreactors are then discussed in a greater detail. Then, it introduces two types of photobioreactors that were used in this work. Next chapters present individual computational models for hydrodynamics and mass transfer, respectively. These chapters also present preliminary work that was done to develop and set-up these models. Furthermore, the models are complemented with laboratory experiments so that the results could be validated, as well. At last, results of each model are discussed in respective summaries.

In addition to the hydrodynamic and mass transfer models, there is a brief demonstration of an additional irradiation model at the end of the thesis. Lastly, final conclusions are discussed and some future work is proposed.

2 METHODS IN MODELING OF PHOTOBIOREACTORS

2.1 COMPUTATIONAL MODELS OVERVIEW

A large number of flows encountered in nature and industry are mixtures of phases. Advances in computational fluid mechanics have provided the basis for further insight into the dynamics of multiphase flows. Therefore, the applicability of CFD methods to such flows has become common practice in engineering. Among the available multiphase simulation approaches for hydrodynamic studies, the Eulerian–Eulerian (E-E) and the Eulerian–Lagrangian (E-L) multiphase models have been popularly used.

The Eulerian–Eulerian multiphase model averages the Navier–Stokes equations over the control volume and solves the continuity, mass, and momentum equations for a combination of fluid phases or fluid and solid phases. It considers all phases in the Eulerian representation, creating the need for mass and momentum balances for each phase. This approach uses only one pressure field for all phases and the interaction between phases is modelled through the interaction terms, e.g., the drag force, lift force, wall lubrication force, or turbulent dispersion force. However, their applicability and accuracy in the correct prediction of gas-liquid flow features is different for any considered case. Thus, making this multiphase approach rather complex. For example, flow in bubble columns is driven by the rising bubbles so the main interfacial forces are buoyancy, drag, lift, and virtual mass. In case of the flow agitated by the stirrer, buoyancy and drag forces seem to dominate (Buffo and Marchisio, 2014).

The comprehensive modelling approach of a photobioreactor should include four sub-models and a coupling method (Gao et al., 2018). The interplay between sub-models is schematically shown in Figure 2.1. Only the multiphase fluid dynamics model and the species mass transport model will be presented in this work.

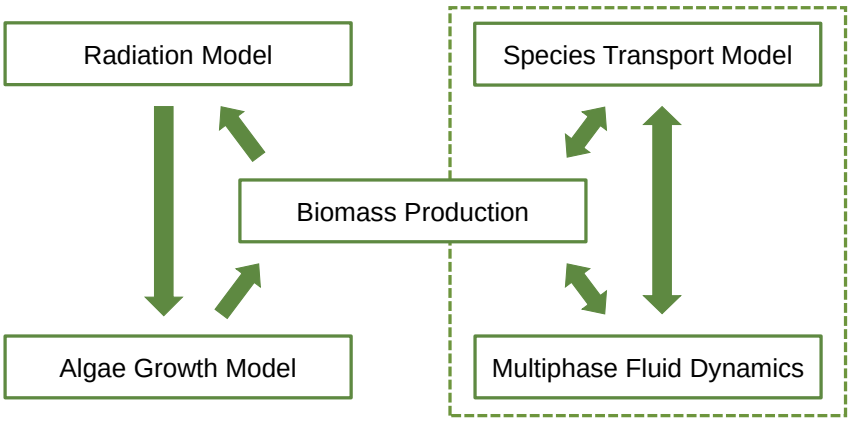

Figure 2.1 Scheme of the comprehensive photobioreactor model

As a result, to study the characteristics of a culturing systems in photobioreactors with all sub-models combined is a rather complex task. Therefore, the majority of the studies puts focus only on a specific component of the photobioreactor model (Pires et al., 2017). Moreover, very little research has been focused on full-scale photobioreactors for mass cultivation. This is mainly due to the difficulties in maintaining internal environmental conditions of the full-scale photobioreactors, producing a similar light intensity and spectrum as sunlight, and evaluating the mixing efficiency according to the different photobioreactor designs (Seo et al., 2012).

2.1.1 Gas-liquid hydrodynamics

In the photobioreactor technology, the gaseous phase serves primarily as a nutrient for cells. However, it can also affect mixing of the medium (Bitog et al., 2014). Therefore, bubbles can have an impact on a variety of chemical and biochemical reactions that take place in the vessel (Almani et al., 2021). Often, the strategy is to study bubbly flow at the level of a single bubble and apply the findings and set-up to subsequent, more complex, flow studies (Ziegenhein and Lucas, 2017).

Depending on the medium and the flow regime, bubbles can have various forms of shapes. Therefore, a problem can arise when defining the bubble size in terms of a single diameter. Hence, there are different approaches to define the equivalent bubble diameter in the literature. Dijkhuizen et al. (2010) based the bubble equivalent diameter on the horizontal and vertical diameter, d_h and d_v respectively, that were obtained in an experiment with the PIV set-up. Ziegenhein and Lucas (2017), on the other hand, took the major and minor axis of the projected bubble area. The equivalent bubble diameter was then defined as the spherical equivalent of the rotational volume. In the work of Thobie et al. (2017), the equivalent diameter corresponds to the diameter of a spherical bubble having the same projected area as the measured bubble. However, this approach may result in an overestimation of the real equivalent diameter in case of large bubbles which are flattened in the column gap.

2.1.2 Gas-liquid mass transfer

Understanding the gas-liquid mass-transfer process in (photo)bioreactors is a key to improved reactor designs and reactor operation as they are important to maximize efficiency and minimize costs. Because of the low solubility of most gases, the gas–liquid mass transfer often becomes the rate-limiting step for the overall reaction (Linek et al., 1996). Typically, a bioreactor for gas treatment is operating under mass transfer or kinetically limited conditions. Understanding the rate-limiting steps in such system, therefore, gives opportunities to optimize the design and operations of the system for a specific application.

The overall mass-transfer coefficient is a combination of a series of partial mass-transfer coefficients, e.g., mass transfer rate coefficient for the gas phase (k_G), the

mass transfer rate coefficient for the liquid phase (k_L), and the mass transfer rate coefficient for the biofilm (k_B). Furthermore, since the k_L coefficient is the most dominant, other coefficients are often neglected. The k_L coefficient is usually modulated by the specific gas–liquid interfacial area a. Thus, producing the volumetric mass-transfer coefficient $k_L a$. However, the liquid-side volumetric mass-transfer is difficult to estimate as it is affected by many factors, e.g., gas hold-up, bubble size, slip velocity and turbulent energy dissipation rate. Moreover, these factors are also depended on reactor operating conditions, geometry, and physical properties of the gas and liquid phases (Gao, 2016).

The models used the most often in works related to (photo)bioreactors are the Penetration model (Higbie, 1935) and the Eddy cell model (Lamont and Scott, 1970). The Penetration model, Eq. (1), assumes unsteady mass transfer only when a liquid element is in contact with bubbles and at equilibrium at the gas-liquid interface. The model is also characterised by the fact that each liquid element is in contact with the gaseous phase for the same time. In contrast to that, the Eddy cell model, Eq. (2), predicts the mass transfer based on the interfacial surface renewal by small scale eddies.

$$k_L = \mathrm{F}\sqrt{\frac{4D_L u_{slip}}{\pi d_b}} \tag{1}$$

$$k_L = \mathrm{K}\sqrt{\frac{4D_L}{\pi}\sqrt{\frac{\varepsilon_L}{\nu_L}}} \tag{2}$$

2.2 PHOTOBIOREACTORS

Following text presents two photobioreactor types, the flat-panel photobioreactor and tubular photobioreactor. These vessels were used for work in this dissertation thesis and were placed at the Institute of Process Engineering at Faculty of Mechanical Engineering at Brno University of Technology.

2.2.1 Flat-panel photobioreactor

The hydrodynamic model assessment of the flat-panel photobioreactor was performed on the lab-scale cuvette. This cuvette was of a stirred flat-panel type with dimensions in Figure 2.2. The cuvette's back wall could be lit with a LED array. Its interior was equipped with a U-shaped stainless-steel aerator tube, Teflon-coated stir bar, and two Ø 12 mm probes, a pH probe and a temperature probe.

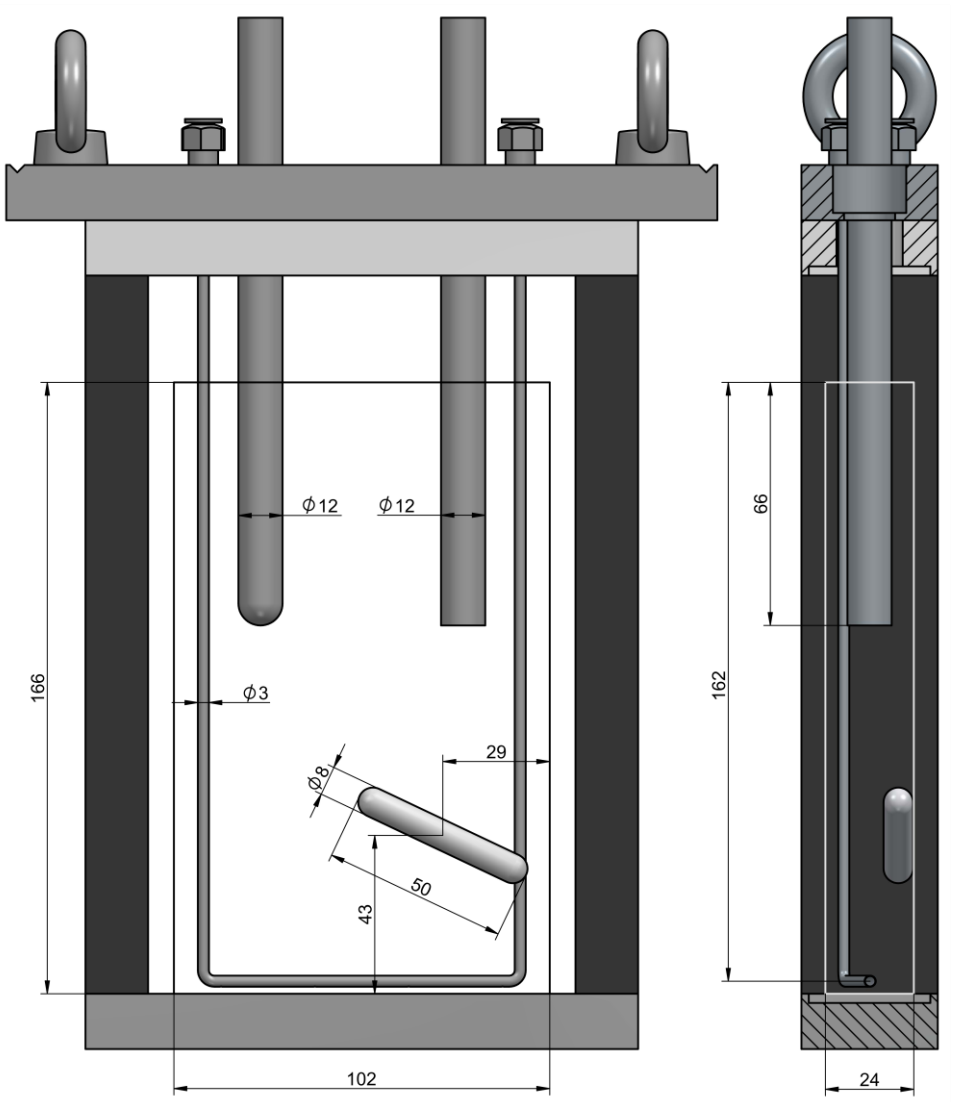

Figure 2.2 Orthographic view of the cuvette within its frame and with dimensions. The figure does not show glass panels. The rectangle marks its inner volume instead where the its height is limited to the water free surface.

The U-shaped aerator tube delivered air near the cuvette bottom through four Ø 0.7 mm holes. The stir bar was of a magnetic type and was placed at the front glass panel inside the vessel. There was no shaft that would introduce some features to the cuvette's glass panels so it could be easily exchanged or removed. Possible rotational speeds for the motor were between 120 and 600 revolutions per minute (rpm) yielding the Reynolds number in the range of 5,000 and 25,000, respectively. In addition to the temperature probe, the temperature could be controlled by a Peltier cell in the cuvette's base. The aeration gas flow through the cuvette was controlled by a flow controller and could reach up to 300 ml min^{-1} where the aeration gas was air enriched by 3 % CO_2. The flow of both phases inside the photobioreactor was affected by the stirrer and/or air sparging. The stirrer-induced agitation formed the most intensive flow patterns that were able to break bubbles. Under non-agitated conditions, i.e., in a bubble rising regime, the bubbles could be as large as 5 mm in diameter and mostly of ellipsoid shape. This shape was also dominant under the low agitation speeds.

2.2.2 Tubular Photobioreactor

For preliminary analyses of the mass transfer phenomena in photobioreactors, the vertical bubble-column cultivation system was used. In this cultivation system, there were three main parts:

- two gas storage tanks,
- a buffer tank,
- three vertical tubes.

The reactor vessel itself was made from three vertical tubes with a rectangular cross-section of dimensions 44x20 mm and rounded corners with 10 mm radius. The tubes were filled with 4.34 litres of water. In total, 105 litres of the aeration gas were fed to the reactor's loop from storage tanks with composition presented in Table 2.1. The cultivation medium in the reactor's tubes was aerated with the constant total airflow rate of $2\ \mathrm{l\ min^{-1}}$ at 165 mbar from the bottom of the tubes through the perforated inlet membrane. The airflow rate yielded the superficial velocity of $0.013\ \mathrm{m\ s^{-1}}$ placing the bubbly flow into the homogeneous regime (Joshi, 2001) with bubbles uniformly sized and dispersed.

Table 2.1 Aeration gas composition

Species	Amount	
SO_2	50	$\mathrm{mg\ m_N^{-3}}$
CO	50	$\mathrm{mg\ m_N^{-3}}$
NO	200	$\mathrm{mg\ m_N^{-3}}$
O_2	9	$\%_{vol.}$
CO_2	10	$\%_{vol.}$
N_2	81	$\%_{vol.}$

3 HYDRODYNAMIC MODEL

This chapter presents the hydrodynamic model used in the lab-scale cuvette. It describes the experimental methods used for flow measurements in the laboratory, the numerical model for computer simulations, and their results. At first, the experimental method is presented. Next, the hydrodynamic multiphase numerical model is introduced with its results presented comparably to the experiments. At last, a critical summary is given at the end of the chapter.

3.1 EXPERIMENTAL WORK

The Particle Image Velocimetry (PIV) system by Dantec Dynamics at the Technical University of Liberec was used for velocity measurements. The system consisted of a NewWave Gemini pulsed laser with 10 ns pulse length and frequency of 532 Hz. The images were captured by 5.5 Mpx Dantec Neo camera with a 50 mm focal length lens

and 500 frames per second shutter speed. The experimental setup with the cuvette is in Figure 3.1. The velocity field was measured in a vertical plane through the centre of the cuvette. However, in case of two-phase flow measurement without agitation, the cuvette was equipped only with the U-shaped aerator tube. In case of other measurements, the cuvette was fully equipped and in order to eliminate shadows from the suspended probes, the laser beam had to be split to form two coplanar laser planes. This setup then resulted in an inability to measure the region between the probes. Therefore, the data from this part were not used for the flow validation.

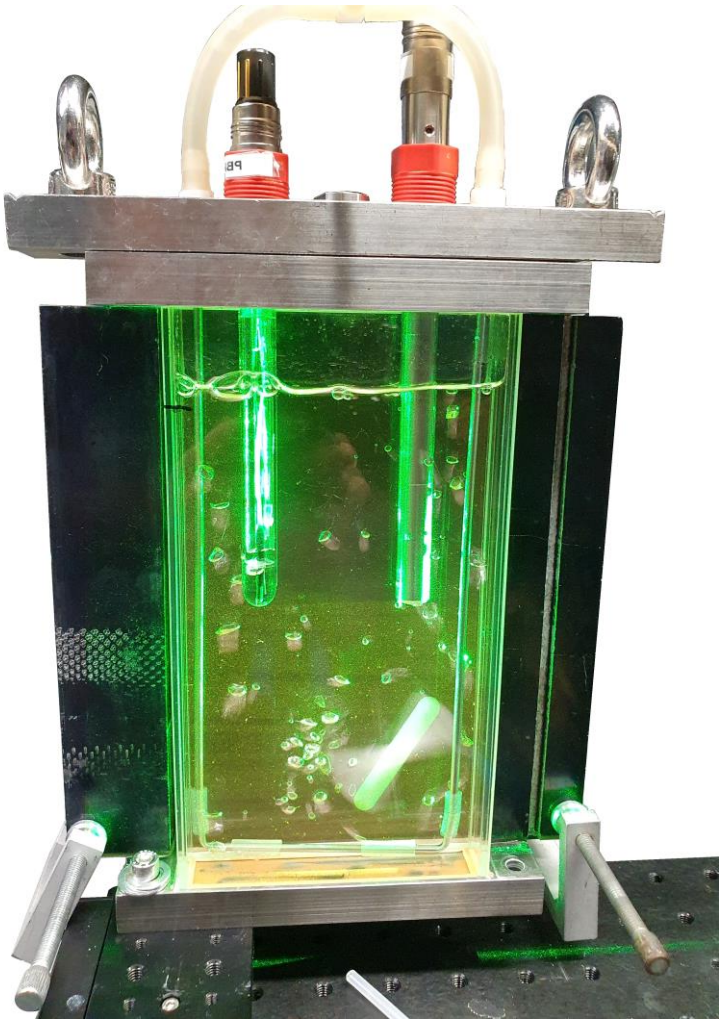

Figure 3.1 Experimental PIV setup – cuvette filled with water is aerated, agitated, and lit with laser planes.

The water was seeded with 20 μm polyamide particles coated with a rhodamine layer. Reflection of light from the walls and accessories was eliminated using optical filters suitable for the wavelength emitted by the particles. Post-processing of the data was performed in the Dynamic Studio software. This included cross-correlation algorithms for the computation of velocity vector maps. Additionally, bubble rising velocities were calculated by tracking bubbles in digital images taken by the high-speed camera.

To measure the fluid flow depending on the operational regime, following step-by-step analysis was performed:

- Two-phase flow measurement with flow induced by bubbles only
- Single-phase flow measurement with flow induced by stirrer only
- Two-phase flow measurement with flow induced by stirrer and bubbles

3.2 NUMERICAL SIMULATIONS

The CFD model was based on the two-fluid approach within Eulerian–Eulerian (E-E) framework with constitutive closures for interphase forces and liquid turbulence. The two-fluid environment was made from the liquid water and the gaseous air. Since the photobioreactor was generally operated at 20 °C, the corresponding values of material properties used in numerical simulations were the default values in the ANSYS Fluent, i.e., 998.2 kg m^{-3} in density and 1.003 mPa·s in viscosity for the liquid water, and 1.225 kg m^{-3} in density and 0.0179 mPa·s in viscosity for the injected gaseous air. The air-water surface tension is 0.072 N m^{-1}.

All phases combined in the E-E framework formed interpenetrating continua where the amount of each phase was determined by the volume fraction. The framework used a single pressure field that was shared among all phases. Momentum equations were calculated for the continuous and every dispersed phase separately, i.e., each phase had its own velocity field. Moreover, the turbulence was modelled in all simulations. Since the k-ε family of turbulence models was used the most often in simulations of photobioreactors, its latest modification known as the Realizable k-ε Turbulence Model together with the Enhanced Wall Treatment was also considered in this work. Regarding the multiphase character of the flow and low gas volume fraction (ca. 0.6 %), the dispersed formulation of the turbulence model was employed, i.e., only the turbulence for the continuous phase was modelled. Turbulence modelling on the dispersed-phase side was possible with turbulence interaction terms.

Regarding the phase interaction models, only the drag force modelling was included. The Grace drag model was selected as it is recommended for bubbles that can have different sizes and shapes (ANSYS Inc., 2020). The applicability of suitable drag models was studied in Rebej et al. (2020). Other interaction models, e.g., lift force or virtual mass force, were not considered in simulations. The effect of such models was not found to bring any improvements in results. Moreover, the convergence and numerical stability was negatively affected.

Nevertheless, the numerical model used the Phase Coupled SIMPLE algorithm to couple the phasic momentum equations, the continuity equation, and the phasic volume fraction equations. The spatial discretization for pressure field was employed with the Body Force Weighted scheme and the First Order Upwind scheme for the volume fraction equation. Other variables used the Second Order Upwind scheme. All numerical analyses were solved in the transient solver. Convergence was considered

on the basis of residuals, levels below 10^{-3} were required. The time-step size varied between different sets of analyses.

In terms of operating conditions, the effect of the gravitational acceleration was included in the model. Moreover, to capture the buoyancy of the gaseous phase, the operating density was set to the density of air with the operating pressure of 101,325 Pa at the water free surface, i.e., top of the domain. This surface was treated as the degassing boundary condition, i.e., free-slip wall for the primary phase and the mass-sink for the secondary phase. The interface corresponding to the stationary and rotational zone was treated as the interior boundary. All other walls in the domain had the no-slip boundary condition. The treatment of the gas inlet condition was modelled with the mass-source term in the dedicated cell zones representing the inlet orifices. The cell zones were of the spherical shape with the same diameter as the real-world inlet orifices, i.e., 0.7 mm. The air flow-rate through the photobioreactor was 200 ml min^{-1}.

3.3 RESULTS

The assessment of the multiphase hydrodynamic model was done with means of velocity contours and vector fields from time-averaged values on the cuvette's mid-plane, and velocity profiles in a local coordinate system placed in the main vortex.

Figure 3.2 show velocities in various monitoring points. It can be observed from the figure that the flow has reached its stabilised state. The green area marks the data time-averaging period. Since the simulations were performed for each mesh type (15 simulations in total), and the results of similar cases are to a large extent alike, Figure 3.3 to Figure 3.6 show only the comparison of the PIV results and the mid-plane CFD results with the medium mesh.

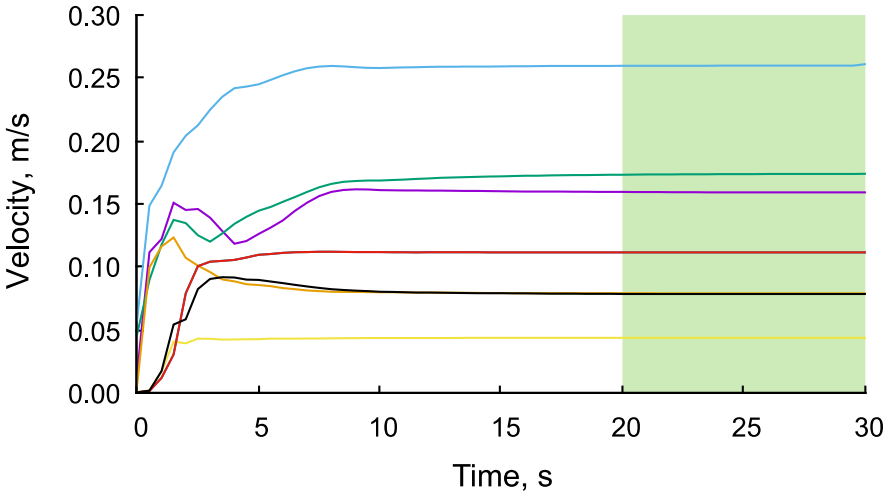

Figure 3.2 Velocity profile from monitoring points inside the domain, 360 rpm and no aeration

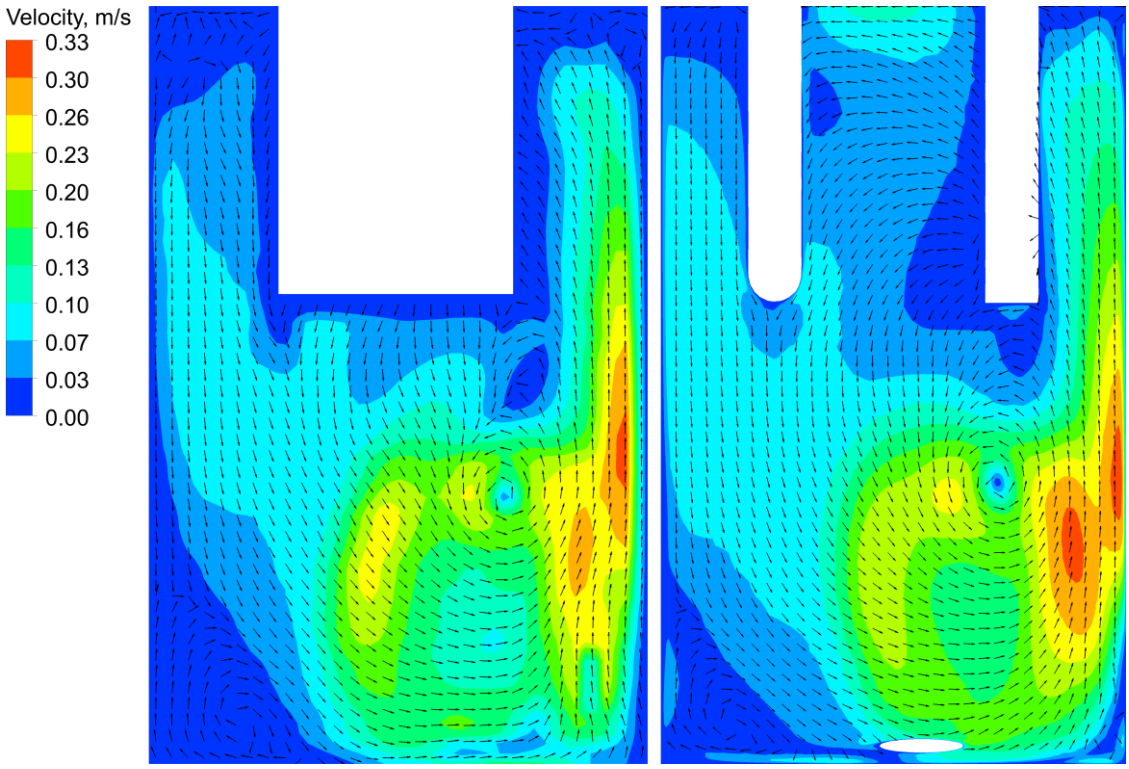

Figure 3.3 Veolcity contour plot, 360 rpm, no aeration;
PIV (left) and CFD medium mesh (right)

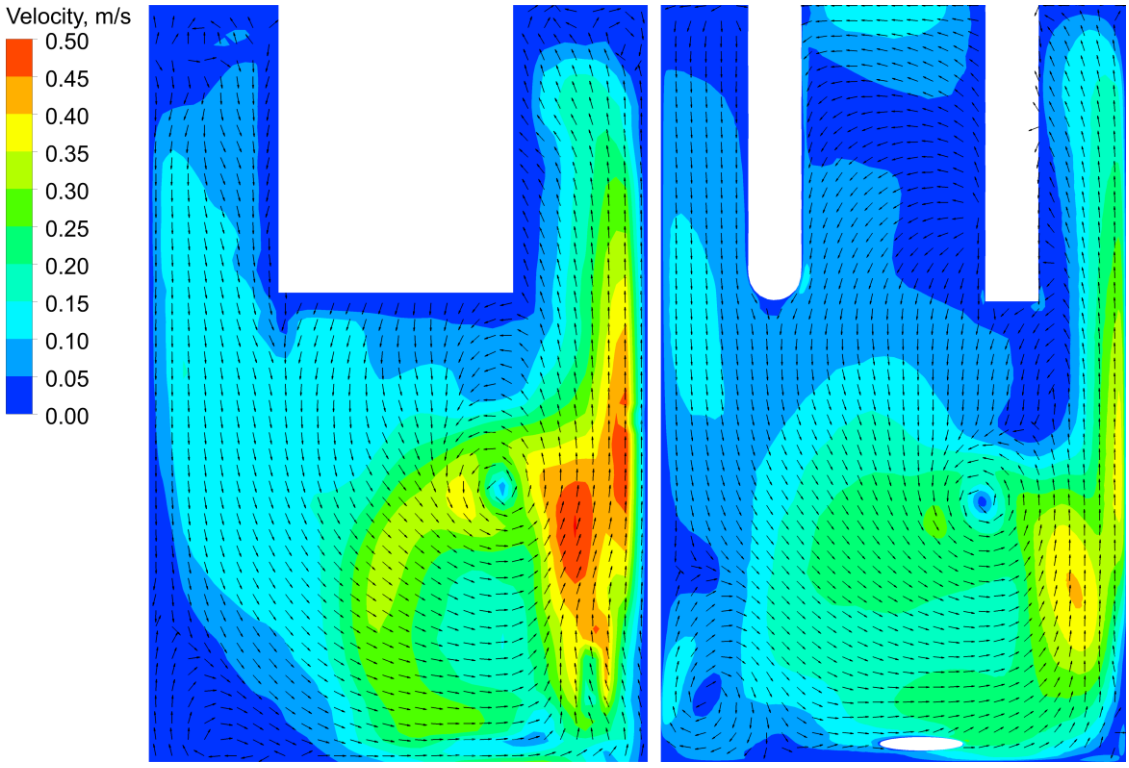

Figure 3.4 Veolcity contour plot, 480 rpm, no aeration;
PIV (left) and CFD medium mesh (right)

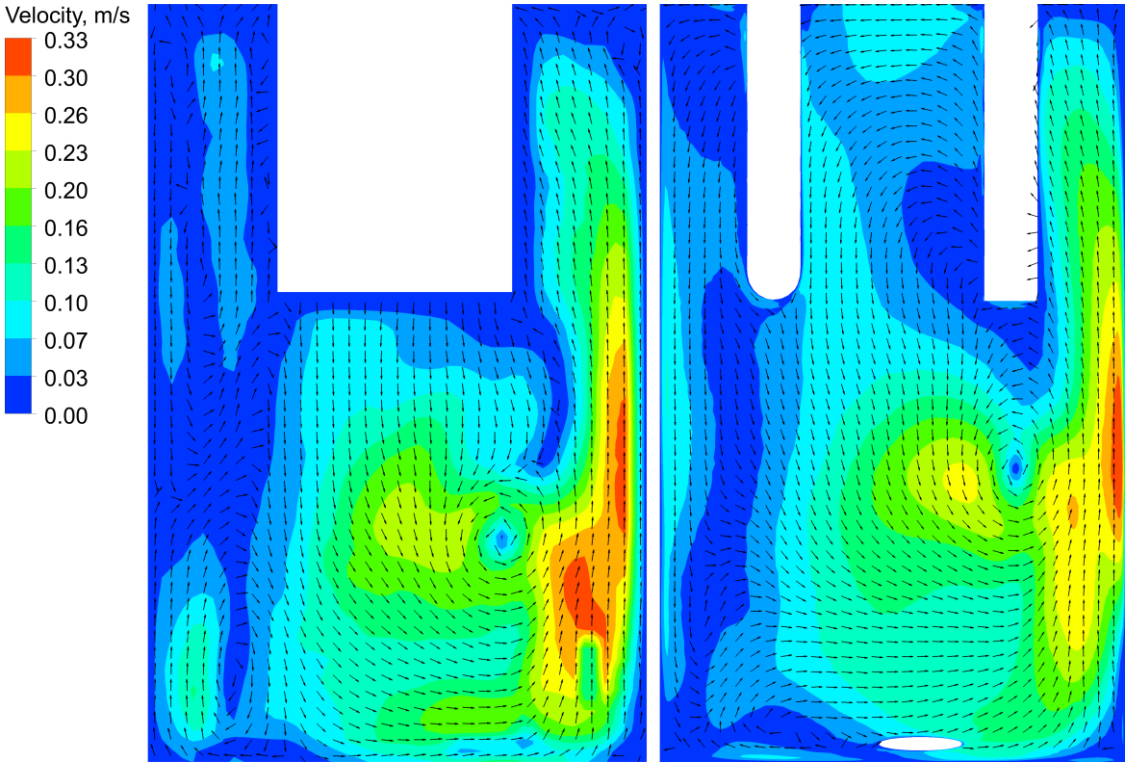

Figure 3.5 Veolcity contour plot, 360 rpm, 200 ml min^{-1} aeration rate; PIV (left) and CFD medium mesh (right)

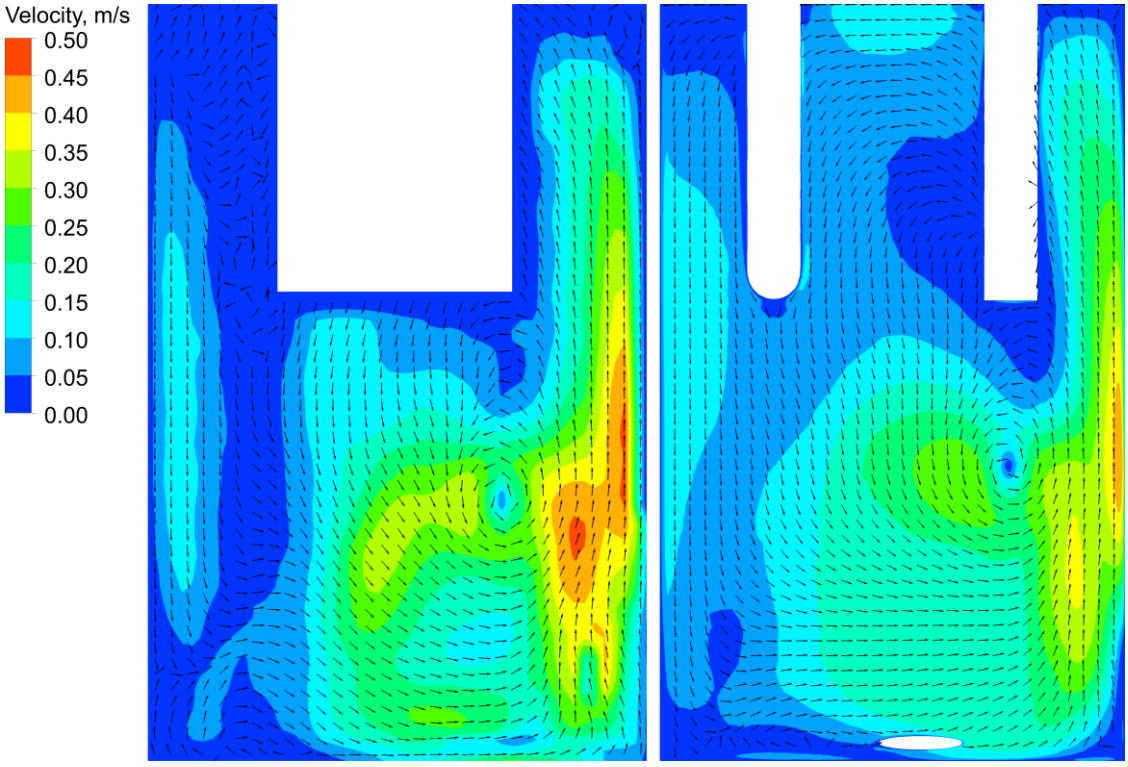

Figure 3.6 Veolcity contour plot, 480 rpm, 200 ml min^{-1} aeration rate; PIV (left) and CFD medium mesh (right)

4 MASS TRANSFER MODEL

Objective in the development of the mass transfer model was to predict the mass transfer coefficient and to validate the numerical results with the experimental data. There were two mass transfer coefficient models implemented into the ANSYS Fluent with the user-defined function, the Penetration model and the Eddy cell model.

4.1 NUMERICAL MODEL

The mass transfer model applied to the flat-panel photobioreactor followed the work that had already been presented, i.e., it used the medium mesh and extended the validated hydrodynamic model. It was also based on the preliminary work on the mass transfer model in the ANSYS Fluent. The reactor was aerated with the aeration gas flow rate of 200 ml min^{-1} and the aeration gas was air enriched with 3 % of CO_2. Experiments were performed with the 360 rpm agitation speed.

The interphase species mass transfer employed the Henry's law formulation. Mass transfer coefficient model constants F and K were obtained by fitting simulation predictions for the Penetration model and the Eddy cell model to the experimental data. Next, in terms of discretization schemes and operating conditions, this setup copied the setup presented in the hydrodynamic model. Similarly, convergence was reached when residuals were below 10^{-3} levels. In addition to that, the approach presented in Ndiaye et al. (2018) was followed so that once the momentum, turbulence, and volume fraction equations were converged and stabilized, their calculation was disabled and the mass transfer was calculated on the frozen hydrodynamic field only. This approach allowed to get the benefit of a larger time step size and to proceed through the required time interval faster. For the expected volume-averaged k_L of $0.4 \cdot 10^{-3}$ m s^{-1}, the time step size of 1 s yielded the CFL of approx. 0.45.

4.2 RESULTS

Laboratory data were provided by the project partner in the form of pH in time. The correlation with the dissolved CO_2 was found with the Cupp et al. (2017). Measured pH values and corresponding saturation of CO_2 in the liquid are presented in Figure 4.1. This laboratory data was used to validate the mass transfer model. In Figure 4.2, the concentration of CO_2 was monitored for both mass transfer coefficient models.

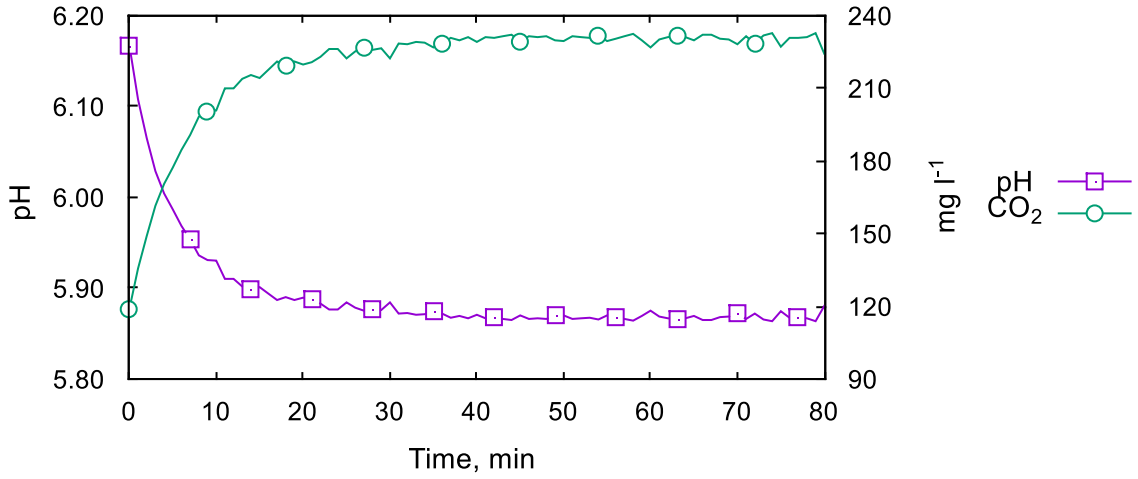

Figure 4.1 Laboratory data

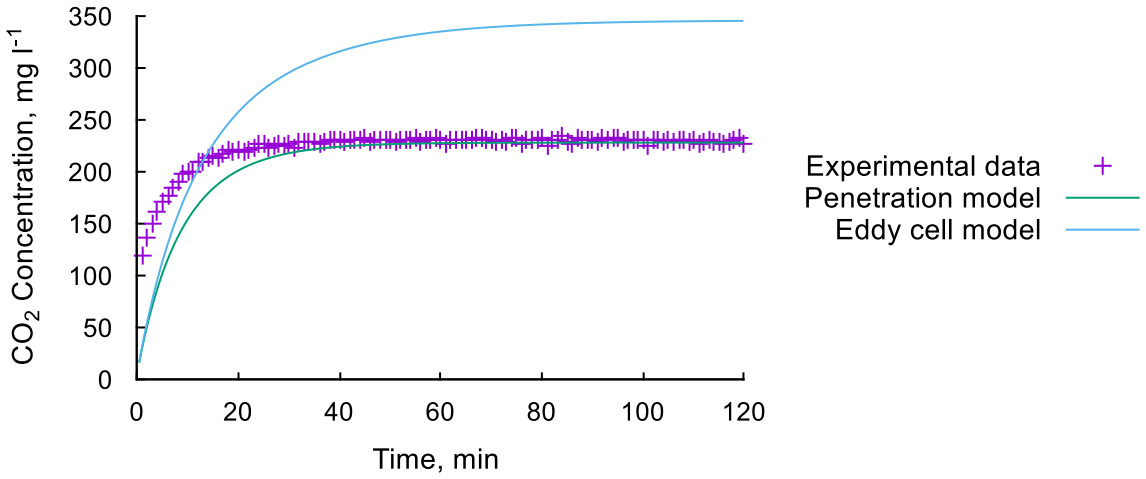

Figure 4.2 CO_2 concentration in the liqud phase

The CO_2 saturation concentration found in the experiment was approx. 235 mg l^{-1} and was predicted the most accurately by the Penetration model. The Eddy cell model overpredicted this value by more than 50 %. The maximum estimated values for the mass transfer coefficient were $0.58 \cdot 10^{-3}$ m s^{-1} and $2.2 \cdot 10^{-3}$ m s^{-1} for the Penetration model and the Eddy cell model, respectively. A detailed contour plots on the cuvette's mid-plane is in Figure 4.3.

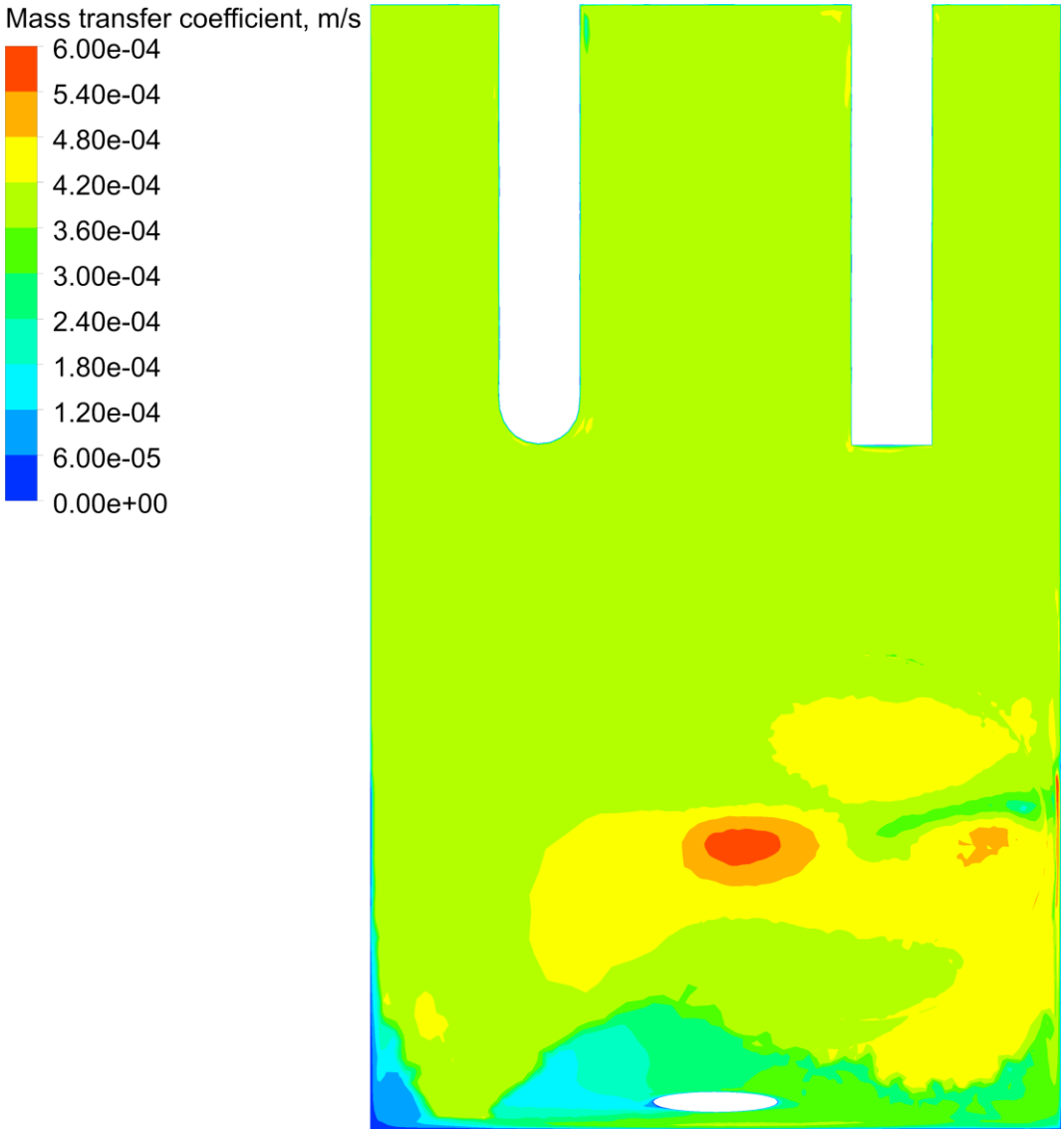

Figure 4.3 Mass transfer coefficient with the Penetration model.

Model constants F and K were specified with values $F = K = 1.0$. These values were selected based on the several mass transfer simulations using the specified model where simulations with different values of the respective model constant were performed. The Penetration model yielded the most accurate results for the $F = 1.0$. However, for a wide range of K values, the Eddy cell model yielded either unrealistic results or its convergence was negatively affected.

The Penetration model showed a good fit in the evolution of CO_2 concentration in the liquid phase of the flat-panel photobioreactor. The volume-averaged mass transfer coefficient was approx. $0.41 \cdot 10^{-3}$ m s^{-1} and, as shown in the Figure 4.3, the model shows uniform distribution of the mass transfer coefficient there. The maximum of $0.58 \cdot 10^{-3}$ m s^{-1} was in the region close to the stir bar where slip velocity was the largest.

5 SUMMARY

My doctoral dissertation thesis dealt with numerical simulations of photobioreactors. The first part of this thesis reviewed the research in numerical modelling of culturing systems. The review presented the most common CFD codes that were used in some recent publications. Essential mathematical models for hydrodynamics, mass transfer, irradiation, and microalgae growth in photobioreactors were summarized there with an overview of the numerical models used in these publications. It was found that authors were often divided in the necessity to include individual meso-scale models that describe the interaction of phases and that the numerical model verification is still crucial for the prospective scale-up applications. Moreover, it was found that there is still a need for a significant development and validation of such sub-models and coupling methods.

The second part of the thesis presented the laboratory photobioreactors used at the Institute of Process Engineering to develop the multiphase hydrodynamic model and the mass transfer model. There were two types of reactors, the flat-panel photobioreactor and the vertical column photobioreactor. The reactors were used for laboratory measurements of the fluid flow and CO_2 absorption, and their computer models were used for numerical simulations.

The Particle Image Velocimetry method was used to measure multiphase velocity fields induced by the stirrer and/or bubbles under different operating conditions in the flat-panel photobioreactor. Comparatively, the multiphase hydrodynamic model of the flat-panel photobioreactor under these operating conditions was developed in the ANSYS Fluent software. The model validation was based on the results of velocity profiles in monitored points, velocity profiles along axes centred to the vortex induced by the rotating stir bar, and velocity contour plots. In addition to that, numerical analyses were carried out on three meshes different in the level of refinement so that the grid independence could be considered. The mesh with the medium level of refinement was considered optimal.

Next part of the thesis covered the species mass transfer model that extended the previously validated multiphase hydrodynamic model. There were two mass transfer coefficient models analysed on both types of photobioreactors discussed. The bubble-column type photobioreactor was used to study time and spatial scales of the problem. Next, the mass transfer model was tailored to the flat-panel photobioreactor type, mainly through its model constants. Its validation was then based on comparison of the absorbed CO_2 in the liquid phase. Finally, the Penetration model-based mass transfer model would be the choice for any future mass transfer simulations.

At last, a brief demonstration of the irradiation model was given. The model was primarily used to test the coupling of individual numerical models in the ANSYS Fluent and to see the possible effect of absorbed CO_2 in the liquid phase on the light distribution. However, the model did not predict any significant changes in the light

attenuation when the CO_2 got absorbed into the liquid phase. The presence of microalgae at concentration greater than 0.5 g l^{-1}, on the other hand, should have a stronger effect (Wheaton and Krishnamoorthy, 2012). At lover concentrations, only internal equipment had significant effect on the light attenuation.

In total, the photobioreactor model presented in the thesis followed the sequence where, at first, the multiphase hydrodynamics model predicted the flow hydrodynamics for both phases, i.e., positional and velocity vectors, specific interfacial area, and volume fractions. Second, the mass transfer model simulated the species transport and mass transfer between gas and liquid species. This yielded the mass transfer coefficient and concentrations of individual species in both phases. Additionally, the irradiation model should simulate the light distribution, i.e., the intensity and scattering with the respect of the CO_2 concentration in the liquid phase.

5.1 FUTURE WORK

The work in this thesis was to develop and validate computational models with an interplay between fluid hydrodynamics and species mass transfer. In addition to that, coupling with radiation transport was demonstrated, as well. Future work should, therefore, include an algae growth model that would predict biomass growth rates needed to determine the performance and scalability of a photobioreactor. Specifically, following work could be done with the current photobioreactor model:

- Analyse shear stresses at different agitation speeds, gas aeration rates, and stirrer sizes
- Extend the gas phase of the multiphase hydrodynamic model with the population balance equation to account for different bubble sizes
- Extend the multiphase hydrodynamic model with the solid phase to account for the microalgae
- Extend the mass transfer model to transfer of other species, e.g. O_2
- Validate the irradiation model with the laboratory experiments
- Link the multiphase hydrodynamic model and the species mass transfer model with the biomass growth model

REFERENCES

Acién Fernández, F. G., Fernández Sevilla, J. M., and Molina Grima, E. (2013). Photobioreactors for the production of microalgae. *Rev Environ Sci Biotechnol* 12, 131–151. doi: 10.1007/s11157-012-9307-6.

Almani, S., Blel, W., Gadoin, E., and Gentric, C. (2021). Investigation of single bubbles rising in Newtonian and non-Newtonian fluids inside a thin-gap bubble column intended for microalgae cultivation. *Chemical Engineering Research and Design* 167, 218–230. doi: 10.1016/j.cherd.2021.01.010.

ANSYS Inc. (2020). ANSYS Fluent Theory Guide, Release 2020 R2.

Bitog, J. P. P., Lee, I.-B., Oh, H.-M., Hong, S.-W., Seo, I.-H., and Kwon, K.-S. (2014). Optimised hydrodynamic parameters for the design of photobioreactors using computational fluid dynamics and experimental validation. *Biosystems Engineering* 122, 42–61. doi: 10.1016/j.biosystemseng.2014.03.006.

Buffo, A., and Marchisio, D. L. (2014). Modeling and simulation of turbulent polydisperse gas-liquid systems via the generalized population balance equation. *Reviews in Chemical Engineering* 30, 73–126. doi: 10.1515/revce-2013-0015.

Cupp, A., Tix, J., Smerud, J., Erickson, R., Fredricks, K., Amberg, J., et al. (2017). Using dissolved carbon dioxide to alter the behavior of invasive round goby. *MBI* 8, 567–574. doi: 10.3391/mbi.2017.8.4.12.

Darpito, C., Shin, W.-S., Jeon, S., Lee, H., Nam, K., Kwon, J.-H., et al. (2015). Cultivation of Chlorella protothecoides in anaerobically treated brewery wastewater for cost-effective biodiesel production. *Bioprocess Biosyst Eng* 38, 523–530. doi: 10.1007/s00449-014-1292-4.

Dijkhuizen, W., van Sint Annaland, M., and Kuipers, J. A. M. (2010). Numerical and experimental investigation of the lift force on single bubbles. *Chemical Engineering Science* 65, 1274–1287. doi: 10.1016/j.ces.2009.09.084.

Gao, X. (2016). Advanced CFD model of multiphase photobioreactors for microalgal derived biomass production.

Gao, X., Kong, B., and Vigil, R. D. (2018). Simulation of algal photobioreactors: recent developments and challenges. *Biotechnology Letters* 40, 1311–1327. doi: 10.1007/s10529-018-2595-3.

Han, S.-F., Jin, W., Tu, R., Abomohra, A. E.-F., and Wang, Z.-H. (2016). Optimization of aeration for biodiesel production by Scenedesmus obliquus grown in municipal wastewater. *Bioprocess Biosyst Eng* 39, 1073–1079. doi: 10.1007/s00449-016-1585-x.

Heo, S.-W., Ryu, B.-G., Nam, K., Kim, W., and Yang, J.-W. (2015). Simultaneous treatment of food-waste recycling wastewater and cultivation of Tetraselmis suecica for biodiesel production. *Bioprocess Biosyst Eng* 38, 1393–1398. doi: 10.1007/s00449-015-1380-0.

Higbie, R. (1935). The rate of absorption of a pure gas into still liquid during short periods of exposure. *Transactions of the American Institute of Chemical Engineers* 31, 365–377.

Joshi, J. B. (2001). Computational flow modelling and design of bubble column reactors. *Chemical Engineering Science* 56, 5893–5933. doi: 10.1016/S0009-2509(01)00273-1.

Lamont, J. C., and Scott, D. S. (1970). An eddy cell model of mass transfer into the surface of a turbulent liquid. *AIChE Journal* 16, 513–519. doi: 10.1002/aic.690160403.

Linek, V., Moucha, T., and Sinkule, J. (1996). Gas-liquid mass transfer in vessels stirred with multiple impellers—I. Gas-liquid mass transfer characteristics in individual stages. *Chemical Engineering Science* 51, 3203–3212. doi: 10.1016/0009-2509(95)00395-9.

Marella, T. K., and Tiwari, A. (2020). Marine diatom Thalassiosira weissflogii based biorefinery for co-production of eicosapentaenoic acid and fucoxanthin. *Bioresource Technology* 307, 123245. doi: 10.1016/j.biortech.2020.123245.

Patnaik, R., Singh, N. K., Bagchi, S. K., Rao, P. S., and Mallick, N. (2019). Utilization of Scenedesmus obliquus Protein as a Replacement of the Commercially Available Fish Meal Under an Algal Refinery Approach. *Frontiers in Microbiology* 10. doi: 10.3389/fmicb.2019.02114.

Pelczar, M. J., Chan, E. C. S., and Krieg, N. R. (1993). *Microbiology*. Tata McGraw-Hill.

Pires, J. C. M., Alvim-Ferraz, M. C. M., and Martins, F. G. (2017). Photobioreactor design for microalgae production through computational fluid dynamics: A review. *Renewable and Sustainable Energy Reviews* 79, 248–254. doi: 10.1016/j.rser.2017.05.064.

Pulz, O. (2001). Photobioreactors: production systems for phototrophic microorganisms. *Appl Microbiol Biotechnol* 57, 287–293. doi: 10.1007/s002530100702.

Ramírez-López, C., Perales-Vela, H. V., and Fernández-Linares, L. (2019). Biomass and lipid production from Chlorella vulgaris UTEX 26 cultivated in 2 m3 raceway

ponds under semicontinuous mode during the spring season. *Bioresource Technology* 274, 252–260. doi: 10.1016/j.biortech.2018.11.096.

Rebej, M., Vondál, J., Juřena, T., and Jegla, Z. (2020). Evaluation of different drag models for simulations of a bubbly flow in a flat-panel photobioreactor. in *Proceedings of the 26th International Conference "Engineering Mechanics 2020"* 1. (Brno University of Technology, Institute of Solid Mechanics, Mechatronics and Biomechanics), 432–435. doi: 10.21495/5896-3-432.

Rodolfi, L., Biondi, N., Guccione, A., Bassi, N., D'Ottavio, M., Arganaraz, G., et al. (2017). Oil and eicosapentaenoic acid production by the diatom Phaeodactylum tricornutum cultivated outdoors in Green Wall Panel (GWP®) reactors. *Biotechnology and Bioengineering* 114, 2204–2210. doi: 10.1002/bit.26353.

Sabeti, M. B., Hejazi, M. A., and Karimi, A. (2019). Enhanced removal of nitrate and phosphate from wastewater by Chlorella vulgaris: Multi-objective optimization and CFD simulation. *Chinese Journal of Chemical Engineering* 27, 639–648. doi: 10.1016/j.cjche.2018.05.010.

Seo, I., Lee, I., Hwang, H., Hong, S., Bitog, J. P., Kwon, K., et al. (2012). Numerical investigation of a bubble-column photo-bioreactor design for microalgae cultivation. *Biosystems Engineering* 113, 229–241. doi: 10.1016/j.biosystemseng.2012.08.001.

Singh, R. N., and Sharma, S. (2012). Development of suitable photobioreactor for algae production – A review. *Renewable and Sustainable Energy Reviews* 16, 2347–2353. doi: 10.1016/j.rser.2012.01.026.

Tanaka, T., Yabuuchi, T., Maeda, Y., Nojima, D., Matsumoto, M., and Yoshino, T. (2017). Production of eicosapentaenoic acid by high cell density cultivation of the marine oleaginous diatom Fistulifera solaris. *Bioresource Technology* 245, 567–572. doi: 10.1016/j.biortech.2017.09.005.

Thobie, C., Gadoin, E., Blel, W., Pruvost, J., and Gentric, C. (2017). Global characterization of hydrodynamics and gas-liquid mass transfer in a thin-gap bubble column intended for microalgae cultivation. *Chemical Engineering and Processing: Process Intensification* 122, 76–89. doi: 10.1016/j.cep.2017.10.009.

Wheaton, Z. C., and Krishnamoorthy, G. (2012). Modeling radiative transfer in photobioreactors for algal growth. *Computers and Electronics in Agriculture* 87, 64–73. doi: 10.1016/j.compag.2012.05.002.

Ziegenhein, T., and Lucas, D. (2017). Observations on bubble shapes in bubble columns under different flow conditions. *Experimental Thermal and Fluid Science* 85, 248–256. doi: 10.1016/j.expthermflusci.2017.03.009.

CV

Personal Information	
Name	Ing. Miroslav Rebej
Birth date	19.11.1993
Citizenship	Slovak
Education	
Period	09/2019 → (ongoing)
Institution	Faculty of Mechanical Engineering
	Brno University of Technology
Field	Doctoral studies, Design and Process Engineering
Period	09/2016 – 06/2019
Institution	Faculty of Mechanical Engineering
	Brno University of Technology
Field	Master studies, Process Engineering
Period	08/2017 – 12/2017
Institution	Norwegian University of Science and Technology
Field	Erasmus+ Exchange Programme
Student Internships	
Period	07/2018 – 09/2018
Institution	Plzeňský Prazdroj Slovensko, Brewhouse Šariš
Period	07/2017 – 08/2017
Institution	Adient Slovakia
Period	02/2015 – 08/2016
Institution	Hestego a.s., Vyškov CZ

ABSTRACT

Simulations of photobioreactors with microalgae-specific cultures is a field that connects microbiology with the multiphase fluid dynamics. With microalgae cultivation, it is necessary to account various phenomena, e.g., multiphase hydrodynamics with water, CO_2 bubbles and microalgae, multiphase species mass transfer, radiation transport, light attenuation, growth and culmination of microalgae and their effect on fluid properties. Computational model presented in this doctoral dissertation thesis links multiphase hydrodynamic model and the species mass transfer model. In the thesis, there is an overview of applicable computational models for the given types of photobioreactors. The multiphase hydrodynamic model and the species mass transfer model then draw from this overview. Next, the accuracy of these sub-models was compared with laboratory experiments. As a result, the developed computational model of the photobioreactor can be further extended with other sub-models, i.e., the irradiation model and the biomass growth model.

ABSTRAKT

Modelování fotobioreaktorů s kulturami specifických mikrořas je oborem, který propojuje mikrobiologii s vícefázovou mechanikou tekutin. Při kultivaci je nutné zohlednit řadu jevů, jako např. vícefázové proudění zahrnující vodu, bubliny CO_2 a mikrořasy, vícefázový přenos látek, přenos energie zářením, intenzitu pohlcování světla či růst a množení mikrořas a jejich vliv na vlastnosti tekutiny Výpočtový model prezentován v téhle doktorské dizertační práci právě propojuje vícefázový hydrodynamický model s modelem přenosu hmoty jednotlivých složek. V práci je uveden základní přehled výpočtových modelů aplikovatelných pro různé typy fotobioreaktorů. Z tohoto přehledu pak bylo vytvořeno finální nastavení vícefázového hydrodynamického modelu a modelu přenosu hmoty jednotlivý složek. Přesnost výpočtových sub-modelů pak byla ověřena pomocí laboratorních experimentů. Ve výsledku tak může být vyvinutý výpočtový model fotobioreaktora dále rozšířen o další výpočtové sub-modely, a to o model záření a model růstu mikrořas.